



A THEORETICAL AND EXPERIMENTAL COMPARISON OF THE EQUIVALENT SOURCE METHOD AND A BAYESIAN APPROACH TO NOISE SOURCE IDENTIFICATION

Antonio Pereira, Quentin Leclère and Jérôme Antoni
Laboratoire Vibrations Acoustique, INSA Lyon
antonio.pereira@insa-lyon.fr
25 bis avenue Jean Capelle, 69621, Villeurbanne Cedex, France

ABSTRACT

Noise source identification and quantification based on field measurements performed by a microphone array is an usual task in many fields of acoustical engineering. Several approaches have been developed in order to tackle this problem, for example, beamforming, near-field acoustic holography (NAH), inverse methods such as equivalent source method (ESM) and the inverse boundary element method (IBEM), to cite only a few. Depending on the problem configuration (nature of the source field, frequency range of interest and the operational conditions) one method is often preferred over the others. Recently, a Bayesian approach combining physical and probabilistic information was proposed to solve acoustic source reconstruction problems. The deduction of a particular regularization mechanism and a criterion to select the regularization parameter depending on the probabilistic assumptions about the source field is a significant feature of this approach. The aim of this paper is to provide a theoretical and experimental comparison between Bayesian approach and the ESM to deal with a noise source identification problem.

1 INTRODUCTION

The design of a product that emits noise often requires an acoustic adjustment either to adhere to a regulation or specification, or to improve its acoustic performance. A common approach to solve this problem is by means of noise source identification and quantification techniques, which aim to characterise the emitted noise and consequently provide appropriate design changes. Several methods have been developed to perform this task, for instance, beamforming [4], spherical harmonics beamforming [7], near-field acoustic holography (NAH) [14, 15], vector intensity reconstructions based on NAH [16], inverse method such as the inverse boundary

element method (iBEM) [10] and the equivalent source method (ESM) [9, 12, 13]. These methods are based on discrete field measurements generally provided by a microphone array and on an extrapolation step, where the sound field is back propagated up to a desired surface. Depending on the problem characteristics (e.g. nature of the source field, frequency range of interest or operation conditions) one method is often preferred over the others. Recently, a Bayesian formulation of the inverse problem was proposed to sound source reconstruction applications [2], where all the unknown quantities of interest are considered random variables and a cost functional is constructed by combination of physical and probabilistic information. Furthermore, one of the main features of the Bayesian approach is the deduction of a particular regularization mechanism and new criteria to select the regularization parameter. Our interest in this paper is to provide a theoretical and experimental comparison between the Bayesian approach and the equivalent source method to solve a noise source reconstruction problem. The ESM is an inverse problem which principle is to replace a given acoustic field by the superposition of fields generated by a set of equivalent sources. In other words, the idea applied here is to relate the acoustic pressure measured by a microphone array to a distribution of elementary sources representing a discretization of a source surface, by means of a propagation matrix. As well-known, this is often an ill-posed problem requiring regularization and the selection of a good regularization parameter is a key aspect to this problems. The generalized cross-validation (GCV) and the L-curve criterion are commonly applied to this task and several publications had addressed the issue of finding an optimal regularization parameter in vibration and acoustics applications [5, 11, 13]. Firstly, the theory of ESM and the Bayesian approach will be briefly introduced and a comparison by means of a numerical simulation and an experimental application will be presented.

2 OUTLINE OF THEORY

2.1 Equivalent Source Method (ESM)

ESM is based on the idea of modeling an acoustic field by a superposition of waves generated by a set of elementary sources. Given that M measurement points are sampled by a microphone array and a set of N equivalent sources are distributed on a source surface, the direct problem can be expressed in a matrix form as:

$$\mathbf{p} = \mathbf{G}_{(M \times N)} \mathbf{q}, \quad (1)$$

where \mathbf{p} is a column vector with the measured acoustic pressure, \mathbf{q} is a column vector with the strength of equivalent sources and \mathbf{G} is a complex transfer matrix obtained from a Green's function, which is assumed to be known. Our interest in this paper is the case where the number of equivalent sources is always larger than the number of measurement points, i.e. $M < N$ (underdetermined case). A standard way to solve underdetermined problems in linear algebra is by means of the right pseudo-inverse $\mathbf{G}^{+R} = \mathbf{G}^* (\mathbf{G}\mathbf{G}^*)^{-1}$ of the matrix \mathbf{G} , where the superscript $*$ indicates Hermitian transpose (conjugated transpose). This approach provides, among the infinite number of solutions, the solution of minimum norm. However this inversion is often ill-posed, thus requiring regularization to find a useful and stable solution (i.e. less sensitive to perturbations in \mathbf{p}). In order to apply Tikhonov regularization to this problem, Eq. (1) can be written in terms of the singular value decomposition (SVD) of \mathbf{G} :

$$\mathbf{p} = \mathbf{G}\mathbf{q} = \mathbf{U}_{(M \times M)} \mathbf{S}_{(M \times M)} \mathbf{V}_{(M \times N)}^* \mathbf{q}, \quad (2)$$

in which \mathbf{S} is a diagonal matrix with singular values, the columns of \mathbf{U} are the left singular vectors and the columns of \mathbf{V} the right singular vectors such that $\mathbf{U}^* \mathbf{U} = \mathbf{I} = \mathbf{V}^* \mathbf{V}$. The regularized solution is obtained by the inverse of Eq. (2) and introducing the regularization parameter β in the following equation:

$$\mathbf{q}_\beta = \mathbf{V}(\mathbf{S}^2 + \beta^2 \mathbf{I})^{-1} \mathbf{S} \mathbf{U}^* \mathbf{p}, \quad (3)$$

which corresponds to the following minimization problem:

$$\mathbf{q}_\beta = \text{Arg min} \{ \|\mathbf{p} - \mathbf{G}\mathbf{q}\|_2^2 + \beta^2 \|\mathbf{q}\|_2^2 \}, \quad (4)$$

where the regularization parameter β controls the weight given to the minimization of the two terms, i.e. the residual norm $\|\mathbf{p} - \mathbf{G}\mathbf{q}\|_2^2$ and the solution norm $\|\mathbf{q}\|_2^2$. The aim is to find a good compromise between the two terms via a suitable value of β such that the regularized solution is useful and fits the measured data well enough. Therefore, the selection of an optimal regularization parameter is a key aspect of Tikhonov regularization. Several approaches are available to determine the parameter value, for instance the generalized cross validation (GCV) [6] and the L-curve criterion [8].

2.2 Bayesian Approach

Hereafter, the theoretical background of the Bayesian approach will be briefly described. Readers are referred to the papers [1–3] for further details. The model used here is similar to the one used in Sec. 2.1, however, written in its continuous form with an additional term \mathbf{n} representing the measurement noise:

$$\mathbf{p} = \int_S q(\mathbf{r}) \mathbf{G}(\mathbf{r}) dS(\mathbf{r}) + \mathbf{n}, \quad (5)$$

where $\mathbf{p} \in \mathbb{C}^M$ is a column vector with the measured acoustic pressure. The aim of the inverse problem is to find an estimate of the source field $\hat{q}(\mathbf{r})$ from the measurements \mathbf{p} , which may be written in the form:

$$\hat{q}(\mathbf{r}) = \sum_{k=1}^M c_k \phi_k(\mathbf{r}) = \Phi^T \mathbf{c}, \quad (6)$$

where c_k are coefficients which depend on measurements and ϕ_k spatial basis functions that interpolate the source field. Bayesian inference is used to solve this problem by considering the unknown quantities as random variables that produce a random source field and by seeking its probability distribution $[q(\mathbf{c}, \Phi) | \mathbf{p}]$ conditioned to the observation of the measurements in the vector \mathbf{p} . This is the so-called posterior probability distribution, which may be viewed as a cost functional whose maximization will lead to the optimal parameters $\hat{\mathbf{c}}$ and $\hat{\Phi}$ that best explain the measured data, i.e.:

$$(\hat{\mathbf{c}}, \hat{\Phi}) = \text{Arg max}_{\mathbf{c}, \Phi} [q(\mathbf{c}, \Phi) | \mathbf{p}], \quad (7)$$

which is the so-called maximum a posteriori (MAP) estimates. A closed-form expression for the posterior $[q(\mathbf{c}, \Phi)|\mathbf{p}]$ can be obtained from Bayes' rule:

$$[q(\mathbf{c}, \Phi)|\mathbf{p}] = \frac{[\mathbf{p}|q(\mathbf{c}, \Phi)] [q(\mathbf{c}, \Phi)]}{[\mathbf{p}]}, \quad (8)$$

where the first term on the numerator $[\mathbf{p}|q(\mathbf{c}, \Phi)]$ is the likelihood function, reflecting the probability of observing the measured data \mathbf{p} given the source field $q(\mathbf{c}, \Phi)$, the second term $[q(\mathbf{c}, \Phi)]$ is the a priori probability distribution (“prior”) of the source before the data are measured and the denominator term $[\mathbf{p}]$ is the evidence, which reflects the probability of measuring \mathbf{p} over the whole probability space of the source. A key aspect of the Bayesian approach is the construction of the probability distribution a priori of the source and the likelihood function, which is connected to the model of measurement noise. According to the Central Limit theorem applied to the Fourier transform, the measurement noise in the frequency domain is a circular complex Gaussian random variable with zero mean and covariance matrix $\mathbb{E}\{\mathbf{nn}^*\} = \gamma^2 \Omega_N$, where the matrix structure of Ω_N is known (e.g. spatially white noise, isotropic noise, etc), with normalization $\text{trace}\{\Omega_N\} = M$ so that the quantity γ^2 reflects the mean energy of the noise. Hence, the probability distribution of the likelihood function $[\mathbf{p}|q(\mathbf{c}, \Phi)]$ will be assumed as a circular complex Gaussian.

The choice of the prior probability distribution involves much more flexibility than the likelihood and is connected to any information about the source field that the user has before the experiment is realized. For instance, it could be any spatial information about the radiating regions where the noise is more likely to come from. This information is introduced here by an “aperture function” $\sigma_s^2(\mathbf{r})$ that takes positive or zero values on the source surface. Another prior information could be related to the spatial correlation of the source field. However, in cases where no information about the spatial correlation is available, a common choice is to consider the source field $q(\mathbf{r})$ spatially white in order to obtain a solution with the finest spatial resolution as possible. This choice will lead to the following structure for the spatial covariance function of the random source field:

$$\mathbb{E}\{q(\mathbf{r})q(\mathbf{r}')^*\} = \alpha^2 \sigma_s^2(\mathbf{r}) \delta(\mathbf{r} - \mathbf{r}'), \quad (9)$$

with normalization $\int_S \sigma_s^2(\mathbf{r}) dS(\mathbf{r}) = 1$, so that α^2 reflects the mean energy of the source field, i.e. obtained after integrating the spatial covariance function over the source surface. The probability distribution a priori $[q(\mathbf{c}, \Phi)]$ is assumed to be also a complex Gaussian in this work, although it is remarked that this is not the only possibility.

Since we finally have all necessary probability distributions, the solution of the problem is obtained by maximization of Eq. (8) with respect to the unknown parameters \mathbf{c} and Φ , noting that the maximization also depends on the two unknown hyperparameters γ^2 and α^2 . From [3] we define the following singular value decomposition:

$$\sigma_s^2(\mathbf{r}) \mathbf{G}(\mathbf{r})^* \Omega_N^{-\frac{1}{2}} = \sum_{k=1}^M s_k \phi_k(\mathbf{r}) \mathbf{U}_k^* \quad (10)$$

The reconstructed source field can then be written as [2]:

$$\hat{q}(\mathbf{r}) = \sum_{k=1}^M \frac{s_k}{s_k^2 + \eta^2} \phi_k(\mathbf{r}) \mathbf{U}_k^* \Omega_N^{-\frac{1}{2}} \mathbf{p}, \quad (11)$$

where the parameter $\eta^2 = \gamma^2 / \alpha^2$ reflects a noise-to-signal ratio and the spatial basis functions $\phi_k(\mathbf{r})$ are given by:

$$\phi_k(\mathbf{r}) = \sigma_s^2(\mathbf{r}) \sum_{i=1}^M \frac{\tilde{U}_{ki}}{s_k} \mathbf{G}(\mathbf{r}_i | \mathbf{r})^*, \quad (12)$$

where \tilde{U}_{ki} is the i -th element of the vector $\Omega_N^{-\frac{1}{2}} \mathbf{U}_k$. Equation (12) can be expressed in matrix notation as:

$$\Phi = \sigma_s^2 \mathbf{G}^* (\Omega_N^{-\frac{1}{2}} \mathbf{U}) \mathbf{S}^{-1}. \quad (13)$$

Hence, Eq. (11) can also be written in a matrix form as:

$$\hat{\mathbf{q}} = \Phi (\mathbf{S}^2 + \eta^2 \mathbf{I})^{-1} \mathbf{S} \mathbf{U}^* \Omega_N^{-\frac{1}{2}} \mathbf{p} = \Phi \mathbf{c}. \quad (14)$$

One can note from the results in Eqs. (11) and (14) that Tikhonov regularization appeared in the form of the regularization parameter η^2 . This is a consequence of the probability distribution selected for the prior $[q(\mathbf{c}, \Phi)]$, which in this case was a complex Gaussian. If another type of prior was selected, a different regularization mechanism would appear. Another particularity of the Bayesian approach is the deduction of new criteria to adjust the regularization parameter. One possibility is by assuming that the unknown hyperparameters γ^2 and α^2 are random variables whose probability distribution $[\gamma^2, \alpha^2 | \mathbf{p}]$ has to be maximized after the observation of the measurements \mathbf{p} . This is the idea adopted in this paper, in which the probability distribution a priori of the unknown hyperparameters $[\gamma^2, \alpha^2]$ is considered to be uniform, thus leading to the conclusion that the maximization of the posterior is equivalent to the one of the likelihood, i.e. $[\gamma^2, \alpha^2 | \mathbf{p}] \propto [\mathbf{p} | \gamma^2, \alpha^2]$. The following criterion is obtained [2]:

$$J(\eta^2) = \ln \left(\frac{1}{M} \sum_{k=1}^M \frac{|y_k|^2}{s_k^2 + \eta^2} \right) + \frac{1}{M} \sum_{k=1}^M \ln \left(1 + \frac{s_k^2}{\eta^2} \right) + \ln \eta^2, \quad (15)$$

with $y_k = \mathbf{U}_k^* \Omega_N^{-1/2} \mathbf{p}$. Therefore, the regularization parameter is obtained by minimization of Eq. (15) with respect to η^2 .

2.3 Theoretical comparison

A parallel between the two presented approaches can be drawn from the observation of Eqs. (3) and (14). It can be noted that the main differences are in the computation of the of the spatial basis, the dependence on the covariance matrix of noise for the Bayesian case and how the regularization parameter is estimated. For the sake of comparison, an identical discretization scheme of the source surface is selected for both approaches. Let us now assume that the measurement noise is spatially white (i.e. $\Omega_N = \mathbf{I}$), and the aperture function is uniform on the source surface $\sigma_s^2(\mathbf{r}) = 1$. Thus, we can rewrite Eq. (13) as:

$$\Phi = \mathbf{G}^* \mathbf{U} \mathbf{S}^{-1}. \quad (16)$$

By expanding \mathbf{G}^* in its singular value decomposition form, it follows:

$$\Phi = \mathbf{V} \mathbf{S} \mathbf{U}^* \mathbf{U} \mathbf{S}^{-1}, \quad (17)$$

which can be simplified since $\mathbf{U}^* \mathbf{U} = \mathbf{I}$ and $\mathbf{S} \mathbf{S}^{-1} = \mathbf{I}$, leading to the following relation:

$$\Phi = \mathbf{V}. \quad (18)$$

Thus, for this particular case, the spatial basis obtained from the Bayesian approach are equivalent to the ones from the ESM method. Finally, it can be argued from this relation that ESM may be viewed as a particular case of the Bayesian approach when the prior is assumed to be complex Gaussian, the measurement noise spatially white and the aperture function is uniform on the source surface. The next point left to be compared concerns the determination of the regularization parameter. The L-curve criterion and the GCV are commonly applied to ESM since they do not require any prior information about the measurement noise level or the strength of acoustic sources. In this work we compare the L-curve criterion and the regularization approach resulting from the Bayesian formulation in order to estimate the amount of regularization to be imposed. The comparison is carried out by means of numerical simulations and a experimental application, which results are presented in the next sections.

3 NUMERICAL SIMULATIONS

In this section, a numerical simulation attempting to compare the performance of the L-curve criterion to the proposed Bayesian regularization for the determination of a regularization parameter is presented. The simulation consists of two correlated monopole sources distant by 20 cm. The acoustic pressure is measured by a planar square microphone array with 81 microphones and a constant distance between microphones of 12 cm. The source distribution is defined from the discretization of a square surface (1 m x 1 m) with a constant step of 2 cm. The simulation set-up is sketched in Fig. 1.

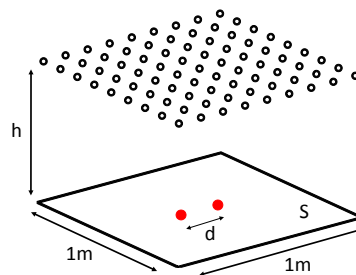


Figure 1: Simulation set-up

The exact pressure field is computed by the direct problem described in the previous section and assuming a free-field propagation. Furthermore, additive and multiplicative white Gaussian noise is added to the simulated measurement pressure. Numerical simulations are carried out

for different signal-to-noise (SNR) levels and for a frequency range of 50 to 2000 Hz with a frequency step of 10 Hz. In order to compare the two approaches objectively, we introduce an indicator based on the knowledge of the exact solution of the problem. Hence, an optimal regularization parameter is defined as the one which minimizes the mean squared error (MSE) between the exact and the regularized solutions for all valid regularization parameters, that is given by:

$$J_{MSE}(\beta) = \|\mathbf{Q}_\beta - \mathbf{Q}_{exact}\|. \quad (19)$$

Four cases are presented in Fig. 2, corresponding to different SNR levels and the array placed at a distance of 20 cm from the source plane. The results correspond to the mean regularization parameter of 100 cases for each SNR and frequency. The average is then normalized by the smallest singular value giving an indication about the amount of regularization that is introduced in the inversion. We observe that the regularization parameter obtained by the L-curve criterion tends to over estimates the optimal regularization at low frequencies and under estimates it in a mid-frequency range depending on the noise level (except for a SNR of 40 dB). These results are in agreement with the ones obtained in Ref. ([13]). On the other hand, the regularization parameter obtained by the Bayesian approach shows a good accordance with the optimal parameter for a wide frequency range and different levels of noise. The results with a 40 dB SNR and frequency range from 1 to 2 kHz correspond to cases where the algorithms hesitate between a regularized or non regularized solution and the determination of a minimum is not stable.

Another indicator is assessed from the computation of the relative error between the regularized solutions and the known exact solution. The errors are computed for each regularization approach and for the non regularized case, their values are obtained by the general expression:

$$\varepsilon(\beta) = \frac{\|\mathbf{Q}_\beta - \mathbf{Q}_{exact}\|}{\|\mathbf{Q}_{exact}\|}, \quad (20)$$

where \mathbf{Q}_β is replaced by the regularized solution of each approach and $\beta = 0$ for the non regularized case. The results are presented in Fig (3) for different levels of measurement noise. As expected, we see that the errors increase when we increase the level of noise and we also notice the sensibility of the inversion, especially at low frequencies. The errors obtained for the Bayesian approach solution are very close to the MSE solution and always inferior than those obtained by the L-curve criterion, unless for the case with 40 dB SNR (1% measurement noise) and high frequencies, where no regularization is seen to be the best option. Interestingly, we also notice that the relative error tends to the level of measurement noise when the problem becomes well-posed, high frequencies in this simulation.

4 EXPERIMENTAL RESULTS

An experimental academic validation was carried out to illustrate the application of the two different approaches for regularization parameter selection. The studied source is a compression driver connected to a tube (22 mm diameter) with three openings (cf. figure 4), constituting three correlated acoustic monopoles. The source is placed in a semi-anechoic room at 20 cm in front of a rectangular 6×5 microphone array, sampling the acoustic field with a constant step

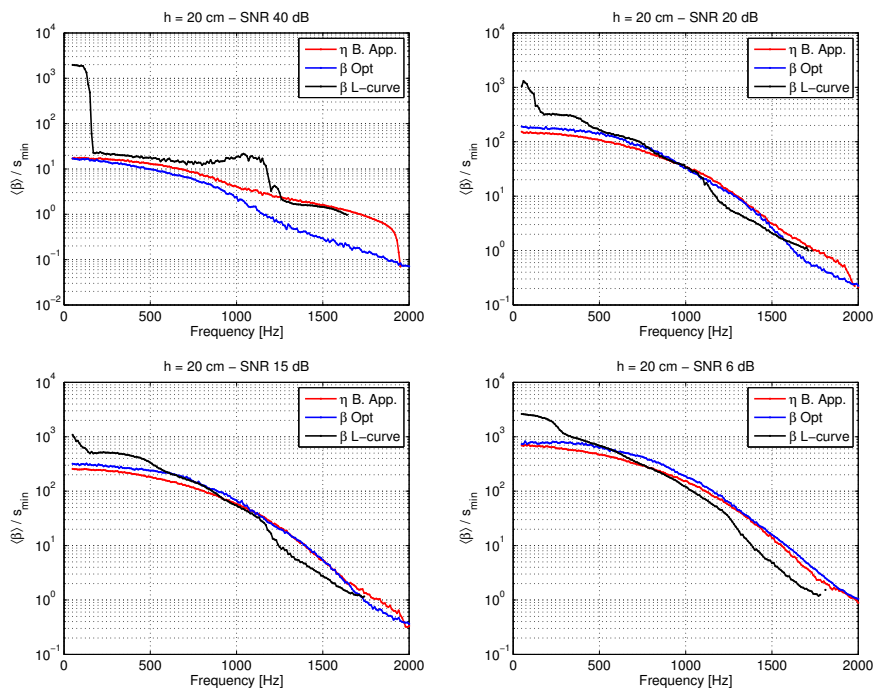


Figure 2: Averaged regularization parameter normalized by the smallest singular value. Top left: SNR 40 dB; Top right: SNR 20 dB; Bottom left: SNR 15 dB; Bottom right: SNR 6 dB

of 10 cm. The virtual monopoles to be identified are distributed on the source plane, over a rectangular surface of 80×70 cm (the microphone array aperture extended by 10 cm on edges), with a resolution of 4 cm. The total number of source DOFs is 483. The validation consists of the reconstruction of the source strength distribution using the regularization approaches examined in Sec. (3).

Firstly, we observe the variation of the selected regularization parameter in function of frequency for both approaches. The results are presented in Fig. 5, with the curvature of the L-curve (normalized by its maximum absolute value at each frequency) on the left and the regularization curve for the Bayesian approach, obtained from Eq. (15), on the right. We can firstly note few discontinuities on the regularization parameter selected by maximization of the L-curve's curvature, for instance, around 600 Hz and 1 kHz. We also observe that, at some frequency bands, more than one local maximum is present, what is related to the discontinuities since at these points the criterion normally changes from one solution to another. On the other hand, the regularization parameter selected by the Bayesian approach evolves in a more continuous manner and there is strictly just one global minimum.

The selected regularization parameters for the two approaches are now plotted on the same graph in function of the frequency to facilitate the comparison (cf. Fig. 6). The source strength distribution for each method is then computed for the particular frequencies marked as vertical lines in Fig. 6. We notice that for 560 Hz, first column of Fig. 7, the L-curve solution is not able to separate the contribution of the two identified sources, contrary to the Bayesian solution.

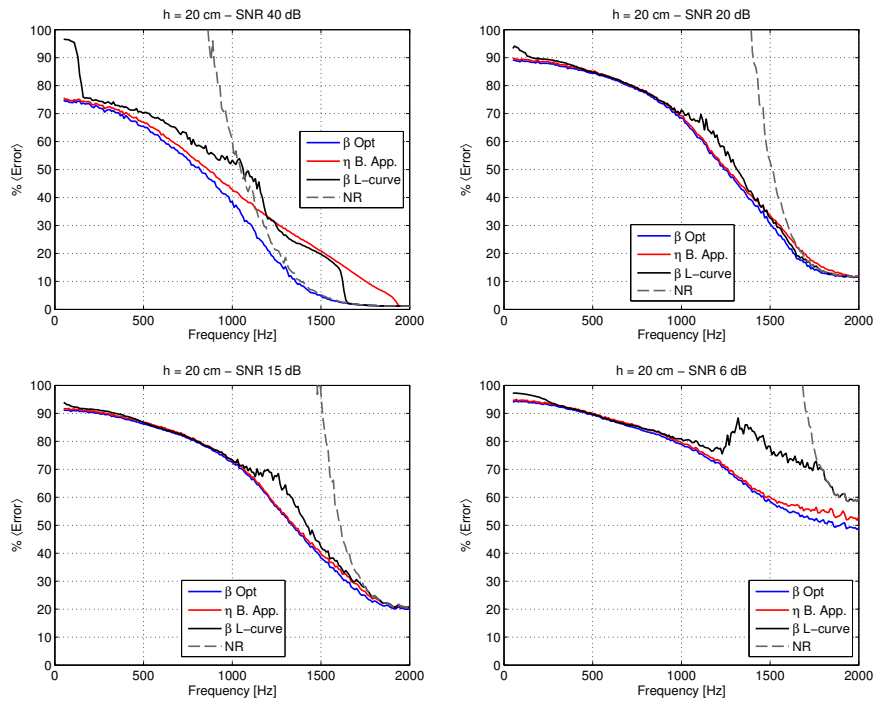


Figure 3: Averaged relative error between the exact and regularized solutions, and for the non regularized solution (NR). Top left: SNR 40 dB; Top right: SNR 20 dB; Bottom left: SNR 15 dB; Bottom right: SNR 6 dB

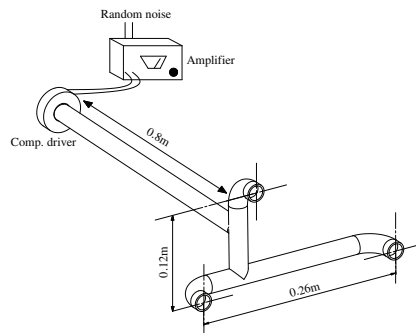


Figure 4: Studied acoustic source.

Furthermore, the reconstructions at 990 Hz, second column of Fig. 7, show that the L-curve solution is more contaminated by ghost sources than the Bayesian solution. At last, the results on the third column of Fig. 7, which correspond to the source reconstruction integrated over the 1-1.2 kHz frequency band, show that the Bayesian solution is slightly less disturbed by ghost sources.

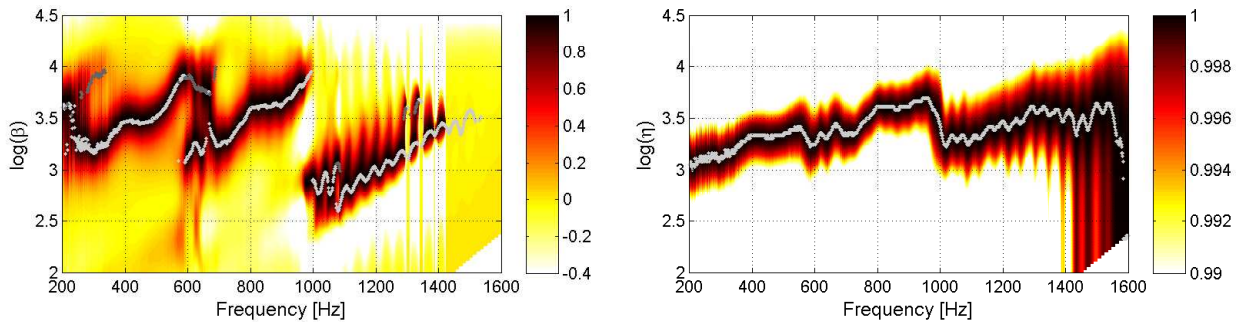


Figure 5: Left: L-curve's curvature in function of frequency and the corresponding regularization parameter which maximizes it. Right: Regularization curve for the Bayesian approach in function of frequency and the respective regularization parameters.

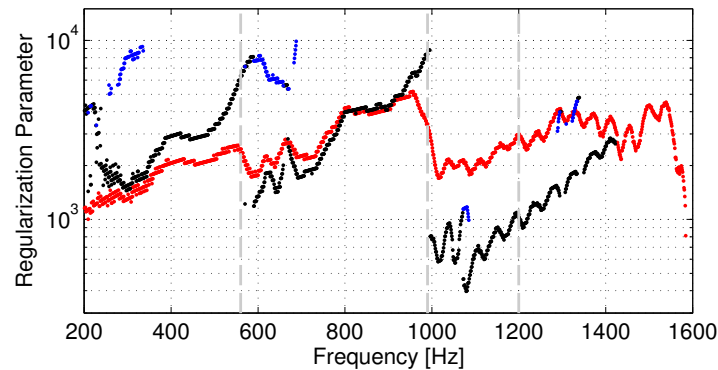


Figure 6: Selected regularization parameters in function of frequency. Bayesian approach (red) and L-curve criterion (black: global maximum, blue: local maximum).

5 SUMMARY

This paper provided a theoretical and experimental comparison between the Equivalent Source Method (ESM) and a Bayesian approach for a source reconstruction problem. It was shown that, under certain assumptions, the solution of the ESM formulation based on the SVD decomposition can be seen as a particular case of the Bayesian approach. Hence, the analysis reduced to the comparison of the performance of methods to estimate regularization parameters for Tikhonov regularization. The L-curve criterion was compared to the regularization approach derived from the Bayesian formulation. The latter has shown the advantage of having no more than one minimum, an attribute that is not usually shared by other approaches. Numerical simulations have been carried out for different levels of measurement noise and a wide frequency range, illustrating that the Bayesian regularization generally gives more satisfactory parameters than the L-curve criterion. Furthermore, an experimental academic validation has confirmed this observation and better reconstruction results were obtained by the Bayesian regularization mechanism.

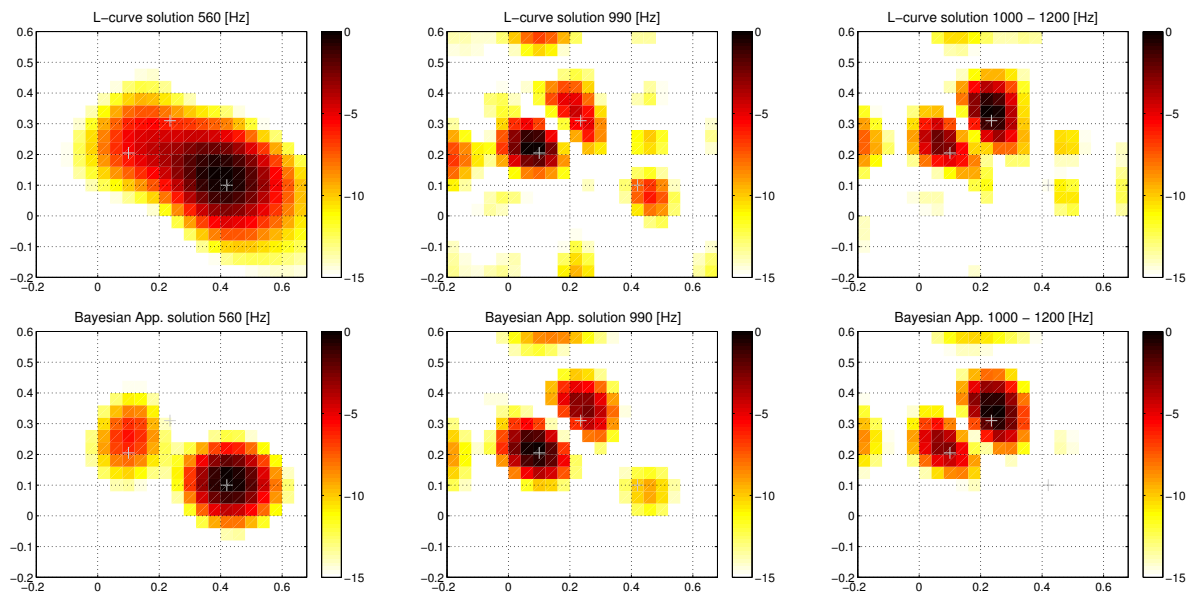


Figure 7: Reconstructed source strength distribution normalized by its maximum value. First row: L-curve based solution. Second row: Bayesian approach solution.

REFERENCES

- [1] J. Antoni. “A bayesian approach to sound source reconstruction: optimal basis, regularization, and focusing.” *accepted for publication in The Journal of the Acoustical Society of America*.
- [2] J. Antoni. “Bayesian focusing: a unified approach to inverse acoustic radiation.” In *Proceedings of ISMA 2010, Leuven, Belgium*. 2010.
- [3] J. Antoni. “Focalisation bayésienne: une approche unifié du problème inverse en acoustique.” In *10ème Congrès Français d’Acoustique, Lyon, France*. 2010.
- [4] J. Billingsley and R. Kinns. “The acoustic telescope.” *Journal of Sound and Vibration*, 48(4), 485 – 510, 1976. ISSN 0022-460X. doi:10.1016/0022-460X(76)90552-6.
- [5] H. G. Choi, A. N. Thite, and D. J. Thompson. “Comparison of methods for parameter selection in tikhonov regularization with application to inverse force determination.” *Journal of Sound and Vibration*, 304(3-5), 894 – 917, 2007. ISSN 0022-460X. doi: 10.1016/j.jsv.2007.03.040.
- [6] G. H. Golub, M. Heath, and G. Wahba. “Generalized cross-validation as a method for choosing a good ridge parameter.” *Technometrics*, 21(2), 215–223, 1979. doi:10.2307/1268518.
- [7] K. Haddad and J. Hald. “3d localization of acoustic sources with a spherical array.” *The*

- Journal of the Acoustical Society of America*, 123(5), 3311–3311, 2008. doi:10.1121/1.2933754.
- [8] P. C. Hansen and D. P. O’Leary. “The use of the l-curve in the regularization of discrete ill-posed problems.” *SIAM J. Sci. Comput.*, 14, 1487–1503, 1993. ISSN 1064-8275. doi: <http://dx.doi.org/10.1137/0914086>.
- [9] R. Jeans and I. C. Mathews. “The wave superposition method as a robust technique for computing acoustic fields.” *The Journal of the Acoustical Society of America*, 92(2), 1156–1166, 1992. doi:10.1121/1.404042.
- [10] B.-K. Kim and J.-G. Ih. “On the reconstruction of the vibro-acoustic field over the surface enclosing an interior space using the boundary element method.” *The Journal of the Acoustical Society of America*, 100(5), 3003–3016, 1996. doi:10.1121/1.417112.
- [11] Y. Kim and P. A. Nelson. “Optimal regularisation for acoustic source reconstruction by inverse methods.” *Journal of Sound and Vibration*, 275(3-5), 463 – 487, 2004. ISSN 0022-460X. doi:10.1016/j.jsv.2003.06.031.
- [12] G. H. Koopmann, L. Song, and J. B. Fahnlne. “A method for computing acoustic fields based on the principle of wave superposition.” *The Journal of the Acoustical Society of America*, 86(6), 2433–2438, 1989. doi:10.1121/1.398450.
- [13] Q. Leclère. “Acoustic imaging using under-determined inverse approaches: Frequency limitations and optimal regularization.” *Journal of Sound and Vibration*, 321(3-5), 605 – 619, 2009. ISSN 0022-460X. doi:10.1016/j.jsv.2008.10.022.
- [14] J. D. Maynard, E. G. Williams, and Y. Lee. “Nearfield acoustic holography: I. theory of generalized holography and the development of nah.” *The Journal of the Acoustical Society of America*, 78, 1395–1413, 1985. doi:10.1121/1.392911.
- [15] W. A. Veronesi and J. D. Maynard. “Nearfield acoustic holography (nah): Ii. holographic reconstruction algorithms and computer implementation.” *The Journal of the Acoustical Society of America*, 81(5), 1307–1322, 1987. doi:10.1121/1.394536.
- [16] E. G. Williams and K. Takashima. “Vector intensity reconstructions in a volume surrounding a rigid spherical microphone array.” *The Journal of the Acoustical Society of America*, 127(2), 773–783, 2010. doi:10.1121/1.3278591.